CNPq

CBPF-CENTRO BRASILEIRO DE PESQUISAS FÍSICAS

Notas de Física

An Effective Liquid Drop Description for the Exotic Decay of Nuclei

by

Marcello G. Gonçalves and S.B. Duarte

Abstract

The present model describes the exotic decay of nuclei including the molecular phase of the fragments by using only the basic elements of the liquid drop fission model. The Coulomb potential energy is the exact solution of the Poisson equation for a uniform charge distribution in the nuclear volume and the surface potential is defined in terms of an effective surface tension. The Werner-Wheeler aproximation for the velocity field of the nuclear flow determines the inertial coefficient of the reduced onedimensional barrier penetrability problem. The model is well succeeded to calculate the half-life of exotic decay process as well as to calculate the alpha desintegration half-life.

Key-words: Surface tension; Gamow penetrability; Half life for exotic and alpha decay.

CBPF-NF-006/93

An Effective Liquid Drop
Description for the Exotic Decay
of Nuclei

by

Marcello G. Gonçalves[1] and S.B. Duarte

Centro Brasileiro de Pesquisas Físicas — CBPF/CNPq
Rua Dr. Xavier Sigaud, 150
22290-180 - Rio de Janeiro, RJ - Brasil

[1]Departamento de Ciências Naturais
Fundação de Ensino Superior de São João del Rei - FUNREI
36300-000 - São João del Rei, MG - Brasil

1 Introduction

Although the discovery of the nuclear fission date of the thirties, the fission process with great mass asymmetry was observed only in the seventies. For the first time this exotic decay was observed at Centro Brasileiro de Pesquisas Ffisicas (CBPF), during a work on U[238] search track fission produts[1,2,3]. Later, other independent experimental observations by Rose and Jones[4] and Alessandrov et. al.[5] confirmed the CBPF pioneering results. Since then, many different models and theoretical estimates have appeared to explain the experimental results and to predict new types of such nuclear processes.

Different nature and forms of the potential has been used in these models[6,7,8,9,10]. The results are led to a reasonable accordance with the observation by adjusting the model parameters. The maximum deviations are within two units around the logarithm of experimental half-live. The number of parameters employed in each model is a consequence of the nature of the potential barrier used [7,8], or it depends on the adopted way in which the mass and charge vary in the prescission phase[8,11]. In addition, it also depends on the empirical method of using the zero point vibrational energy of the system[6,7].

In this work we calculate the half-lives for exotic decays considering a double spherical parametrization for the shape of the deformed nuclear system during the fission process. Although this shape parametrization has been used in others exotic decay models, for the first time we make use of an analytical closed expression to calculate Coulomb energy of the molecular phase of the process. The multidimensional evolution of the system is reduced to the onedimensional case by the geometrical constraints to preserve the adopted shape in the course of the whole process, and also keeping constant the total volume of the system. In the reduced onedimensional problem the Gamow penetrability factor is calculated using an effective mass, determined by using the Werner-Wheeler approximation for the fluid velocity field of the nuclear flow. To complete a basic element of the liquid drop scheme a surface term is included in the potential of the model, with a convenient definition of the surface tension. With only these minimal ingredients of the fission theory in the context of the liquid drop model, we get results in excelent accordance with experimental data for both exotic and alpha decays.

2 The Model : Shape Parametrization and Potential

In the molecular phase of the process the geometrical configuration of the deformed system is approximated by intersecting spheres with different radii. For the complete specification of this configuration it is necessary four independent coordinate, disregarding the location of the center-of-mass of the system. We show in fig.1 a sketch of a generic configuration where we specify our choice of coordinates: the radii of each spherical segment, R_1 and R_2; the height of the largest spherical segment, ξ, and the distance between their geometric centers, ζ. At the end of the prescission phase the system reaches a limiting configuration of two spherical tangent fragments with radii $\bar{R}_1$ and $\bar{R}_2$, respectively, for the cluster emitted and the heavier daughter.

To maintain the adopted shape parametrization for the deformed nuclear system, it

is necessary to establish a geometric constraint,

$$R_1^2 - (\zeta - \xi)^2 = R_2^2 - \xi^2 \quad , \tag{1}$$

keeping a common contact section of the spherical segments during prescission phase. Also the constant total volume of the system is considered as another constraint relation, which is expresed in our coordinates by

$$2(R_1^3 + R_2^3) + 3[R_1^2(\zeta - \xi) + R_2^2 \xi] - [(\zeta - \xi)^3 + \xi^3] = 4 R_p^3 \quad , \tag{2}$$

where R_p is the parent nucleus radius. During the whole molecular phase of fragments we have taken a constant radius to the spherical segment corresponding to the nascent cluster, i. e., we have fixed $R_1 = \tilde{R}_1$.

The model considers only the Coulomb and surface potential energy contributions to the deformation energy of the system. Analytical models for exotic decays have never used before an explicit expression for the coulomb energy during the prescission phase. In the most precise way the Coulomb energy has been taken into account by folding numerically the charge density[6,14] in nuclear volume. In our calculation we have made use of Gaudin expression[12] for the electrostatic energy of spherical portions of uniform charge distribution,

$$V_C = \frac{8}{9}\pi a^5 \epsilon(x_1, x_2) \rho_e \quad , \tag{3}$$

where ρ_e is the initial charge density, ϵ is a function of angular variables x_1 and x_2,

$$x_1 = \pi - \theta_1$$
$$x_2 = \theta_2 - \pi \quad ,$$

which are defined in terms of the angles θ_1 and θ_2, shown in fig.1 .

The expression for the ϵ factor in terms of auxiliary functions f and g is

$$
\begin{aligned}
\epsilon(x_1, x_2) \;=\; & (\frac{1}{\sin^2 x_2} - \frac{1}{\sin^2 x_1}) \left[\frac{f(x_2)}{\sin^2 x_2} - \frac{f(x_1)}{\sin^2 x_1} \right] - \\
& (\cot x_2 + \cot x_1) \left[\frac{f'(x_2) + \frac{\pi}{4}}{\sin^2 x_2} + \frac{f'(x_1) + \frac{\pi}{4}}{\sin^2 x_1} \right] + \\
& \frac{1}{\sin^2 x_1 \sin^2 x_2} \left[f(x_1 + x_2) + \frac{1}{3} \sin^2(x_1 + x_2) \right] + \\
& \frac{\pi}{8} \left[g(x_1) + g(x_2) \right] \;,
\end{aligned}
\tag{4}
$$

where f' is the derivative of f with respect to its argument. Explicitly, the auxiliary functions f, f' and g are given by

$$
f(x) \;=\; 1 - x \cot x - \frac{\pi}{2} \tan \frac{x}{2} \;,
$$

$$
f'(x) + \frac{\pi}{4} \;=\; \frac{2x - \sin(2x)}{2 \sin^2 x} - \tan^2 \frac{x}{2} \;,
$$

$$
g(x) \;=\; \left(1.5 + \tan^2 \frac{x}{2} + 3 \tan^4 \frac{x}{2} \right) \tan \frac{x}{2} + \frac{2}{\sin^3 x} \;,
$$

with x assuming the values appearing as arguments of these auxiliary functions in eq.(4). The above expression of coulomb energy is the exact solution of the Poisson equation for uniform charge distribution in the system volume[12].

For the surface potential we have introduced an effective surface tension, σ_{eff}, to the

-4-

deformed system, defined through the equation

$$\frac{3}{5}e^2\left(\frac{Z_p^2}{R_p} - \frac{Z_1^2}{R_1} - \frac{Z_2^2}{R_2}\right) + 4\pi\sigma_{eff}\left(R_p^2 - \bar{R}_1^2 - \bar{R}_2^2\right) = Q \quad, \tag{5}$$

where $Z_p e$ and $Z_i e$ (i=1,2) are the nuclear charge of the parent nucleus and of the fragments, respectively. This definition establishes that the difference between the energies of initial and final configurations of the system reproduces the energy released in the disintegration, $Q = M - M_1 - M_2$. The masses in the Q–value expression were taken from nuclear data table[15]. Then, for the surface potencial we have,

$$V_s = \sigma_{eff}(S_1 + S_2) \quad, \tag{6}$$

with the surface of each spherical segment,

$$S_i = \pi R_i (R_i + \delta_i) \quad, \tag{7}$$

and

$$\delta_i = \begin{cases} \zeta - \xi & i = 1 \\ \xi & i = 2 \,. \end{cases}$$

The effects of the centrifugal potential in the molecular phase cannot be descussed without a careful analysis of angular momentum transfer in the hydrodinamic flow of the nuclear fluid. In a simplifying approximation all models which take into account this term have considered it only after the scission point,

$$V_\ell = \frac{\hbar^2}{2\bar{\mu}}\frac{\ell(\ell + 1)}{\zeta^2} \quad. \tag{8}$$

In this approximation, the effect of the centrifugal potential to the half-life of exotic decay is completly negligible[16,17]. The reduced mass, $\bar{\mu} = M_1 M_2/(M_1 + M_2)$, defines the rotational inertia of the sytem after scission point.

In fig.2 it is shown our onedimensional potential,

$$V = V_c + V_s + V_\ell - V_0 \ , \tag{9}$$

provide with the constraints given by eqs.(1,2) and with the constant radius of nascent cluster. In the equation above, V_0 means the reference of potential corresponding to the sum of self potential energies (Coulomb and surface) of each fragment in the asymptotic configuration.

3 Gamow Factor and Decay Half-Life

The quantum transition rate from initial to final state of the system has been determined by reducing the problem to the onedimensional barrier penetrability, similarly to Gamow alpha decay theory[13]. Even when the emphasis of the model is on the fission aspects of the process, the decay rate calculation uses the same procedure. The penetrability factor is calculated suposing that the system tunnels a barrier equal to $V - Q$. The shell effects in the nuclear masses expressed in Q-value are reflected in the resulting barrier. Consequently, they are also included in the penetrability factor,

$$\mathcal{P} = \exp\left\{-\frac{2}{\hbar} \int_{\zeta_0}^{\zeta_c} \sqrt{2\mu\left[V(\zeta)-Q\right]}\, d\zeta\right\} \ . \tag{10}$$

The action integral in the penetrability factor is given in terms of the variable of the model, ζ, and the limits are the inner turning point,

$$\zeta_0 = R_p - R_1 \ ,$$

and the outer one

$$\zeta_c = \frac{Z_1 Z_2 e^2}{Q} .$$

Finally, the rate of the decay is calculated as

$$\lambda = \lambda_0 \mathcal{P} .$$

The characteristic time scale of surface oscilations in initial state of the system is used to define barrier assault frequency for the process, λ_0. Swiatecki[19] values of assault frequency with an odd-A parent nuclei hindrance effect,

$$\lambda_0 = \begin{cases} 10^{20} \ s^{-1} & A = odd \\ 10^{22} \ s^{-1} & A = even . \end{cases}$$

were used in present work. With this frequency fixed, the half-life is promptly calculated,

$$\tau = \frac{\ln 2}{\lambda} . \tag{11}$$

4 Radii and Effective Mass

The final radii of the fragments should be given by

$$\hat{R}_i = \sqrt{\frac{Z_i}{Z_p}}\, R_p \ ,$$

(12)

to be consistent with the uniform charge distribution considered in the Coulomb potential. The parent nucleus radius is determined by the simple formula

$$R_p = r_0 A_p^{1/3} \ ,$$

(13)

setting $r_0 = 1.37\ fm$ in all calculations.

With the Werner–Wheeler approximation for the velocity field of nuclear fluid in the prescission phase, we can obtain an expression for the kinetic energy of the system[8,19]. The constraint relations of eqs.(1,2) and a constant radius for the cluster reduce the kinetic energy expression to a quadratic form only in the velocity, $\dot{\zeta}$. From this expression we get the effective mass for the degree of freedom ζ. In the center–of–mass frame we have for this effective mass,

$$m_{eff} = \sum_{i=1,2} \rho_i \left\{ \frac{(z_i')^2\, v_i}{\pi} + 2 \times (-1)^i\, z_i'\, R_i\, R_i'\, (R_i + d_i)^2 \right.$$

$$\left. + \frac{(R_i\, R_i')^2}{2} \left[\frac{4R_i^2}{h_i} - 9R_i - 7d_i + 12R_i \ln\left(\frac{2R_i}{h_i}\right) \right] \right\} \ ,$$

(14)

where the mass density of each spherical segment is $\rho_i = 3M_i/(4\pi R_i^3)$, and

$$z_1' = -\tfrac{1}{2}\left[3v_2 + \pi a^2(R_1 + d_1)\right]/(v_1 + v_2) \qquad z_2' = z_1' + 1$$

$$R_1' = 0 \qquad\qquad\qquad\qquad R_2' = -\tfrac{1}{2}\tfrac{h_2}{R_2}$$

$$d_1 = \zeta - \xi \qquad\qquad\qquad\qquad d_2 = \xi$$

$$h_1 = R_1 - \zeta + \xi \qquad\qquad\qquad h_2 = R_2 - \xi$$

The prime in the above expressions means the derivative with respect to the variable ζ, and $v_i = \tfrac{\pi}{3}(R_i + d_1)^2(R_i + h_i)$ is the volume of each spherical segment. We have used this effective mass as the reduced mass μ in eq.10, defining the penetrability factor. Although the expression for the effective mass changes for different choices of coordinates and frame the result for the decay rate is the same[19]. In fig.3 we show the values of the effective mass of eq.14 for different cluster emission processes. We note that in the limit of asymptotic configurations, this expression for the effective mass reaches the reduced mass of the system when the fragments are already formed, $\bar{\mu}$, as it should be.

5   Results and Discussions

The calculated half-lives of different exotic decays observed in some recent experiments are shown in fig.4 . The thick line of the upper region of the graph corresponds to the calculated result, and the full circles are the logarithm of experimental data compiled in ref.[16]. This result is for zero orbital angular momentum of the fragments. The coresponding reaction and values of half-lives are presented in table-1 . In the table, the reactions with the same cluster emission in exotic process are grouped in blocks. The groups are marked with broken and open arrows in the upper part of fig.4 .

Without any modification in the model only changing the input data for masses, all the calculations were repeated for alpha particle emission of the exotic decay parent nucleus. The results for this essay are presented by the thin line in the lower region of the graph. The numerical values are in the second column of the table-1 . The full

squares are the experimental results compiled in ref.[16]. For alpha decay it should be remembered that angular momentum is not completly negligible for various decays and it might correct some small deviations from experimental data.

In fig.5 we show how sensitive are our results to the effect of the centrifugal potential, including V_ℓ after the prescission point. We can see in fig.5-(a) that the effect is negligible for exotic decay, as it was pointed out before, but it may be significative to the alpha decay, as it is shown in fig.5-(b).

6 Conclusions and Final Remarks

We have analyzed the half-life for the exotic decay by using only the basic ingredient of the liquid drop fission theory. The Coulomb energy was calculated analyticaly for the molecular phase of the system, with a double intersecting spheres parametrization for the deformed nuclear system.

The Werner-Wheeler approximation for the velocity field of nuclear fluid in the prescission phase defines the mass coefficient in the Gamow factor of the onedimensional barrier penetrability calculation.

The effective character of the model is marked by the surface tension defined in eq.(5). At this point we have note that nuclear radii are involved in this definition, so the nuclear radius parameter r_0 controls also the intensity of the surface potential. As we are not using explicitly effects of proximity force[16,18] to the potential, we have to compensate it with an appropriated intensity of our surface term. This fact justify our choise of $r_0 = 1.37 fm$. Finally, it is important to remark that we fix this value for all calculations and for both modes of decay presented in our results.

Acknowledgement

Figure captions

Figure 1: Shape parametrization of nuclear deformation. The nascent cluster corresponds to the spherical segment with radius R_1, and the heavier daugther is represented by the spherical segment with radius R_2. The intersection of the spheres is a circle with radius a, and ξ is the distance of the plane of the intersection to the geometrical center of the heavier fragment. The distance between the geometrical centers of the fragments corresponds to ζ.

Figure 2: Onedimensional potential barrier. The coulomb energy is represented by the dotted curve and the long-dashed curve is the surface potential. The total potential is the continuous curve.

Figure 3: Werner–Wheeler effective mass for differents cluster emission as a function of the distance between the geometrical centers of the spherical segments. After the scission point, the effective mass is constant and equal to the reduced mass of the system, $\bar{\mu}$.

Figure 4: Half-lives for the exotic and alpha decay. In the upper region of the graph the thick line is connecting the logarithms of half-life values for the exotic decays listed in table-1. The experimental data are shown by circles, and the arrows atached to the first and last exotic decay data indicate that these values are only lower limits determined experimentally. The error bar for the other data are comparable to the circle size. The thin line in the lower region of the graph connects the results for logarithms of the alpha decay half-life of the parent nuclei of the exotic decay. The data for the alfa decay half-lives are shown by squares, with error bar smaller than the square size.

Figure 5: Half-lives calculated with the centrifugal barrier. The solid line in part-(a), represents the half-life of exotic decays calculated with $\ell = 0\hbar$. The dotted lines represent the half-life calculated with $\ell = 6\hbar$. In part-(b) the results for the same calculation to the alpha decay mode of the exotic decay parent nuclei are shown.
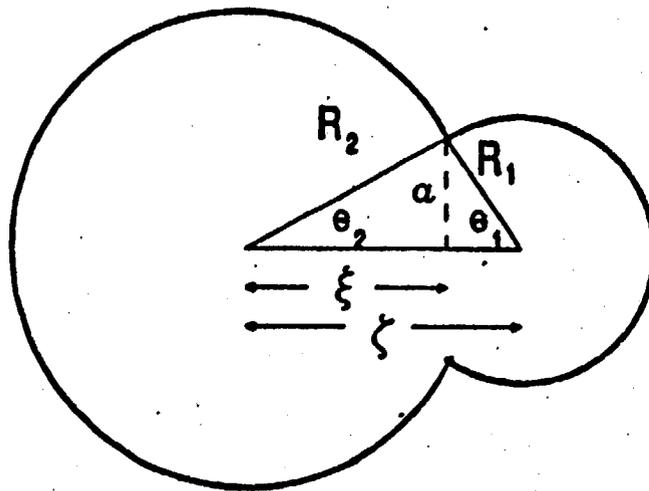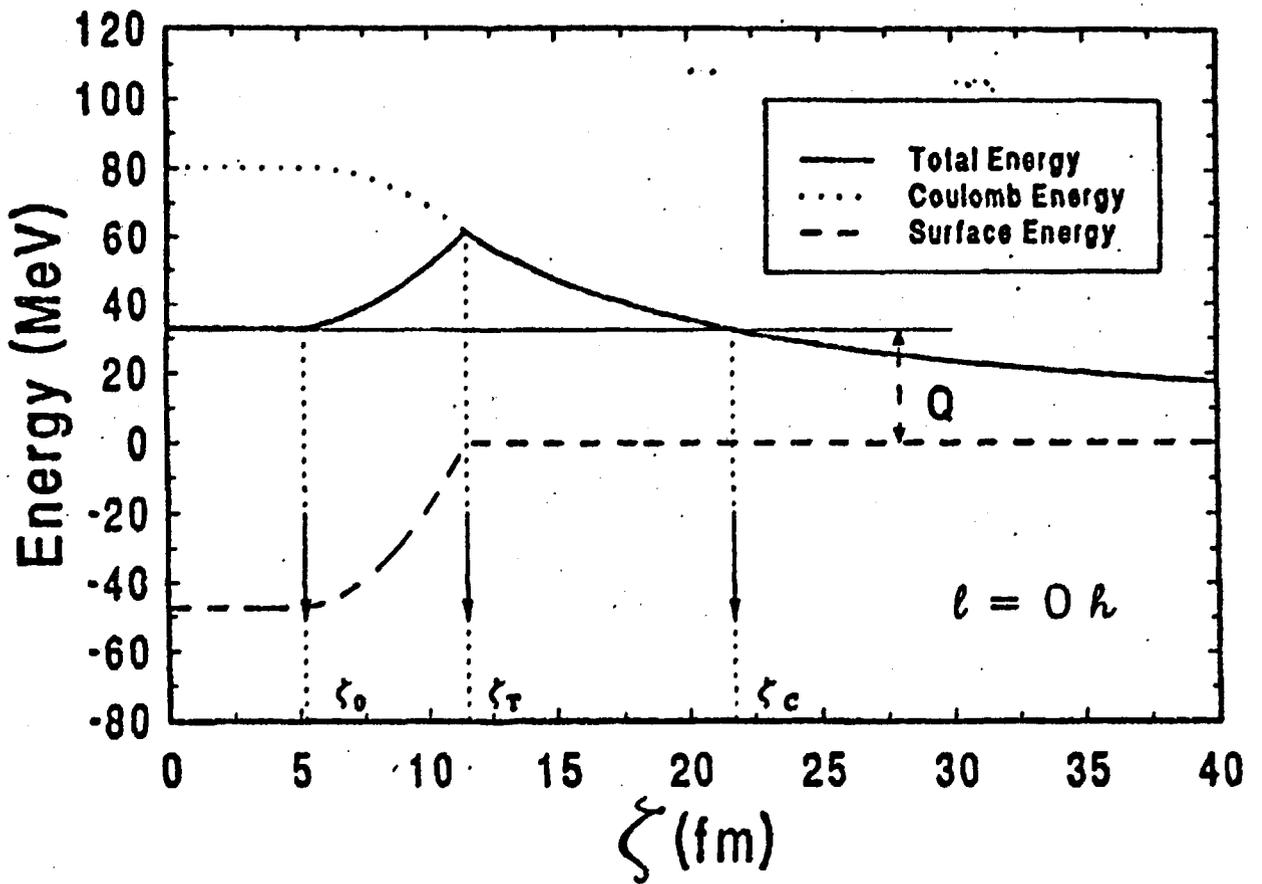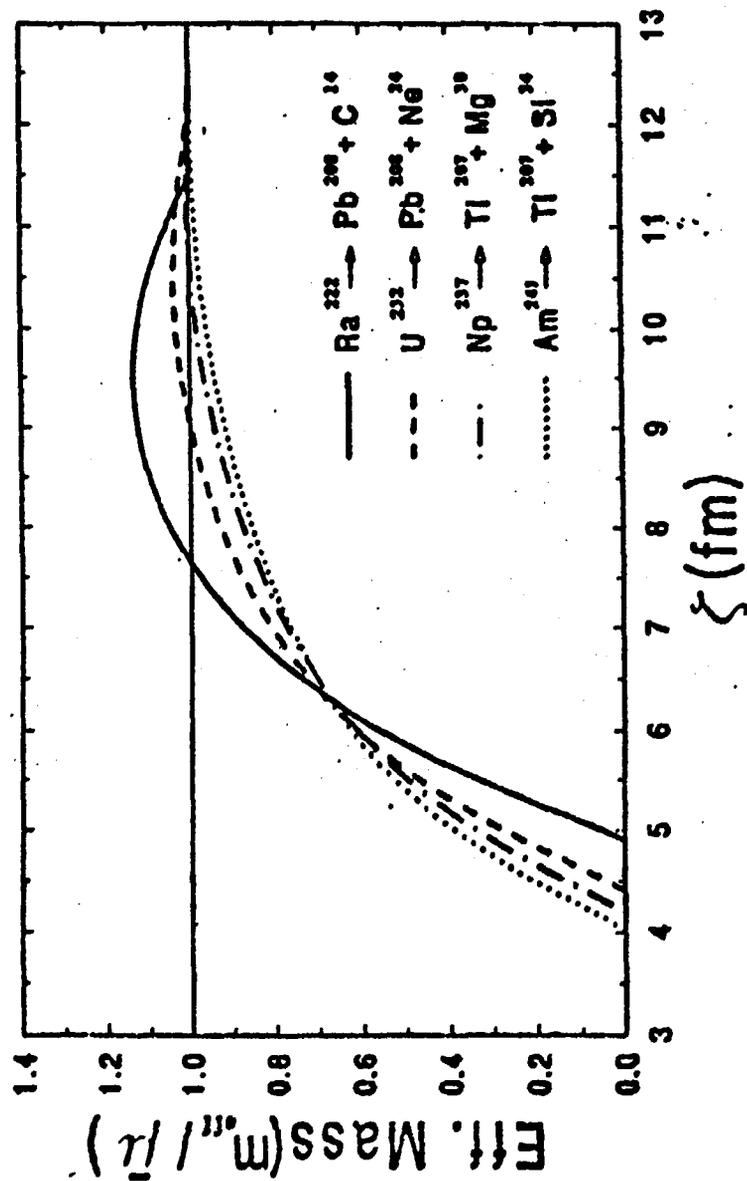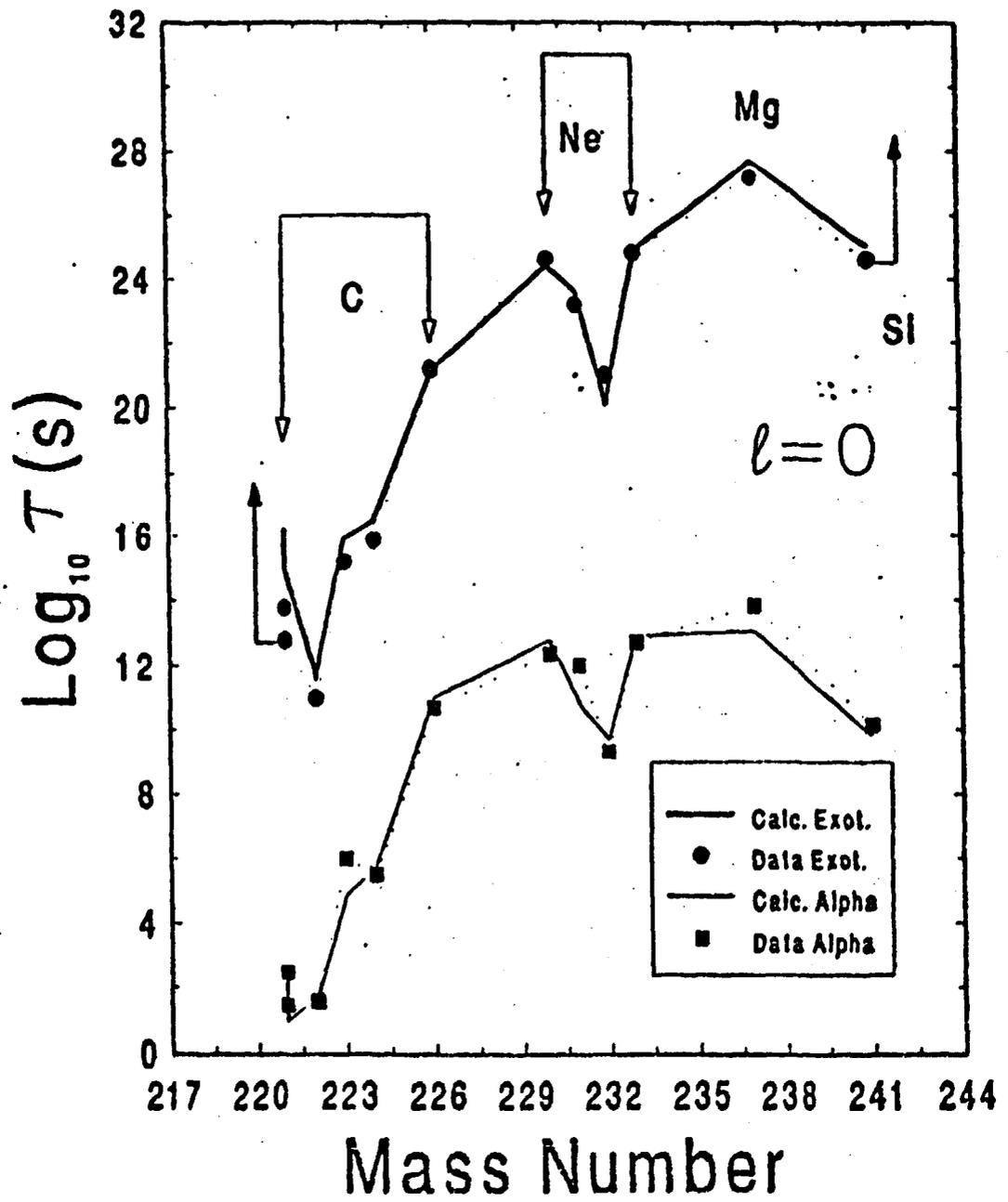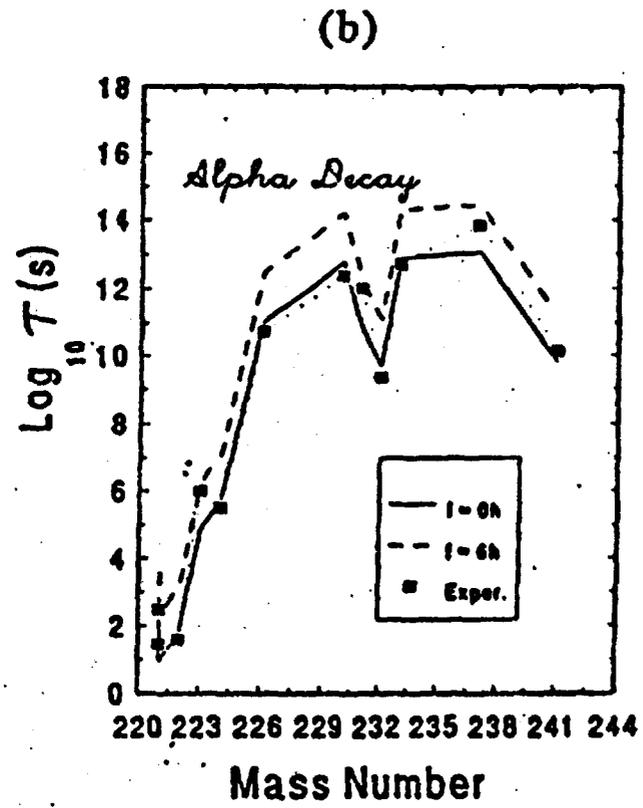
Figure 1

Figure 2

Figure 3

Figure 4

(a)

(b)

Exot. Decay

Alpha Decay

Figure 5
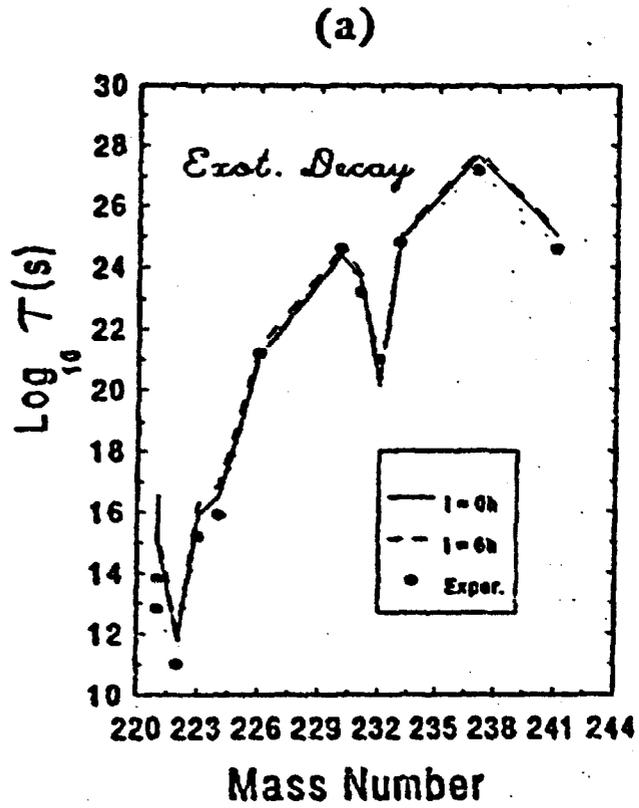
Table and its caption

Decay Reaction	$Log_{10}\tau^{Exot.}(s)$	$Log_{10}\tau^{\alpha}(s)$
$Fr^{221} \rightarrow C^{14} + Tl^{207}$	16.21	2.21
$Ra^{221} \rightarrow C^{14} + Pb^{207}$	14.98	0.95
$Ra^{222} \rightarrow C^{14} + Pb^{208}$	11.72	1.73
$Ra^{223} \rightarrow C^{14} + Pb^{209}$	15.92	4.80
$Ra^{224} \rightarrow C^{14} + Pb^{210}$	16.50	5.73
$Ra^{226} \rightarrow C^{14} + Pb^{212}$	21.09	11.02
$Th^{230} \rightarrow Ne^{24} + Hg^{206}$	24.39	12.76
$Pa^{231} \rightarrow Ne^{24} + Tl^{207}$	23.60	10.80
$U^{232} \rightarrow Ne^{24} + Pb^{208}$	20.10	9.70
$U^{233} \rightarrow Ne^{24} + Pb^{209}$	24.73	12.89
$U^{233} \rightarrow Ne^{25} + Pb^{208}$	24.88	12.89
$Np^{237} \rightarrow Mg^{30} + Tl^{207}$	27.68	13.05
$Am^{241} \rightarrow Si^{34} + Tl^{207}$	25.01	9.79

Table 1: Decay reaction and calculated half-lives. The first numerical column is the logarithm of the exotic decay half-life, and the second one corresponds to the logarithm of the alpha decay half-live of the exotic decay parent nuclei.

References

[1] H. G. de Carvalho, J. B. Martins, I. O. de Souza, and O. A. P. Tavares, An. Acad. Bras. Ciênc. 47, 567 (1975)

[2] I. O. de Souza, M. S. thesis, Centro Brasileiro de Pesquisas Físicas, 1975.

[3] O. A. P. Tavares, Doctoral thesis, Centro Brasileiro de Pesquisas Físicas, 1978.

[4] H. J. Rose and G. A. Jones, Nature 307, 245 (1984).

[5] D. V. Alessandrov, A. F. Belyatskii, Yu. A. Glukhov, E. Yu. Nikol'skii, B. V. Novatskii, A. A. Oglobin, D. N. Stepanov, JETP Lett., 40, 909 (1984).

[6] D. N. Poenaru, M. Ivascu, D. Mazuilu, Comp. Phys. Commun. 19, 205 (1980).

[7] D. N. Poenaru, M. Ivascu, J. Physique 45, 1099 (1984).

[8] Pic-Pichac G. A., Sov. J. Nucl. Phys. 44(6), 923 (1986).

[9] E. Hourani, M. Hussonnois, D. N. Poenaru, Ann. Phys. Fr., 14, 311 (1989).

[10] D. N. Poenaru, W. Greiner, M. Ivascu, D. Mazilu, I. H. Plonski, Z. Phys. A-Atom Nuclei 325, 435 (1986).

[11] G. Shanmugam and D. Kamalaharan, Phys. Rev. C 41, 1742 (1990).

[12] M. Gaudin, Le Journal de Physique, 35 885 (1974).

[13] G. Gamow, Z. Phys. 51, 204 (1928).

[14] B. Buck, A. C. Marchant, S. M. Perez, Nucl. Phys. A 512, 483 (1990).

[15] A. H. Wapstra and G. Audi, Nucl. Phys. A 432, 1 (1985).

[16] Yi-Jin Shi and W. J. Swiatecki, Phys. Rev. Lett., 54, 300 (1985).

[17] H. G. de Carvalho, J. B. Martins, O. A. P. Tavares, Phys. Rev. C 34, 2261 (1986).

[18] Yi-Jin Shi, and W. J. Swiatecki, Nucl. Phys. A 464, 205 (1987).

[19] D. N. Poenaru, J. A. Maruhn, W. Greiner, M. Ivascu, D. Mazilu, I. Ivascu, Z. Phys. A-Atomic Nuclei 333, 291 (1989).